Exact Transient Full-Field Analysis of an Antiplane Subsurface Crack Subjected to Dynamic Impact Loading

Chien-Ching Ma
Professor.

Szu-Kuzi Chen
Graduate Student.

Department of Mechanical Engineering,
National Taiwan University,
Taipei, Taiwan 10764, R.O.C.

The transient problem of a half-space containing a subsurface inclined semi-infinite crack subjected to dynamic antiplane loading on the boundary of the half-space has been investigated to gain insight into the phenomenon of the interaction of stress waves with material defects. The solutions are determined by superposition of the fundamental solution in the Laplace transform domain. The fundamental solution is the exponentially distributed traction on crack faces. The exact close-form transient solutions of stresses and displacement are obtained in this study. These solutions are valid for an infinitely long time and have accounted for the contributions of incident, reflected, and diffracted waves. Numerical results of the transient stresses are obtained and compared with the corresponding static values. The transient solution has been shown to approach the static value after the first few diffracted waves generated from the crack tip have passed the observation point.

1 Introduction

The difficulty in determining the transient stress field in a cracked-elastic body subjected to dynamic loading is a well-known problem. A considerable amount of research has been directed towards the solution of problems involving the interaction of stress waves with the crack and boundary to improve understanding of the behavior of material failure under dynamic loading. The investigation of an idealized semi-infinite crack can provide some information for a realistic elastodynamic fracture problem. It is noted that while the analysis has been carried out assuming a semi-infinite crack, the results remain valid for a finite crack up until the time at which waves diffracted from the far tip reach the tip near the boundary.

In conventional studies of a semi-infinite crack in an unbounded medium subjected to dynamic loading, the complete solution is obtained by integral transform methods together with direct application of the Wiener-Hopf technique (Noble, 1958) and the Cagniard-de Hoop method (de Hoop, 1958) of Laplace inversion. If the loading is replaced by a nonuniform distribution having a characteristic length, then the same procedure using integral transformation methods does not apply. The problem of an elastic solid containing a half-plane crack subjected to concentrated impact loading on the faces of the crack has been previously studied by Freund (1974). He proposed a fundamental solution arising from an edge dislocation climbing along the line ahead of the crack tip with a constant speed to overcome these difficulties of the case with a characteristic length. The solution can be constructed by taking an integration over a climbing dislocation of different moving velocity. Basing his procedure on this method, Brock (1982, 1984, 1985) and Ma and Hou (1990, 1991) have recently analyzed a series problems of a semi-infinite crack subjected to impact loading. Lee and Freund (1990) analyzed fracture initiation of an edge cracked plate subjected to an asymmetric impact.

Whenever dynamic loading is applied to a body with an internal crack, the resulting stress waves may initiate crack growth. Few solutions for a cracked elastic solid subjected to dynamic loading are available. Exact transient close-form solutions for a stationary semi-infinite crack subjected to a suddenly applied dynamic body force in an unbounded medium have been obtained by Tsai and Ma (1992) for the in-plane case and by Ma and Chen (1993) and Brock (1986) for the antiplane case. The problem to be considered in this study is the antiplane response of an elastic half-plane, with an inclined crack extending from infinity to a location near the half-plane surface, which is subjected to dynamic antiplane loading on the half-plane surface as shown in Fig. 1. The propagation of stress waves through an unbounded medium, which are due to applying dynamic loading on the boundary, is not a difficult subject. A pre-existing fault inside the medium would disturb the propagation waves and make the theoretical analysis much more difficult than in an homogeneous medium. In this study, a free boundary and crack are incorporated into the analysis

Contributed by the Applied Mechanics Division of THE AMERICAN SOCIETY OF MECHANICAL ENGINEERS for publication in the ASME JOURNAL OF APPLIED MECHANICS.

Discussion on this paper should be addressed to the Technical Editor, Professor Lewis T. Wheeler, Department of Mechanical Engineering, University of Houston, Houston, TX 77204-4792, and will be accepted until four months after final publication of the paper itself in the ASME JOURNAL OF APPLIED MECHANICS.

Manuscript received by the ASME Applied Mechanics Division, Sept. 30, 1992; final revision, June 12, 1993. Associate Technical Editor: S. K. Datta.

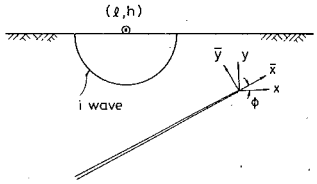

Fig. 1 Configuration, coordinate systems of a subsurface inclined crack subjected to impact loading on the half-space

which made the analysis extremely difficult. In analyzing this problem, the reflections and diffractions of stress waves by the boundary and by the crack which will generate infinite waves, must be taken into account. This problem involves a characteristic length which makes a direct solution by standard techniques difficult. Since none of the methods proposed by Freund (1974) and Brock et al. (1985) have worked for this problem, some other approach must be followed. A new fundamental solution is used for overcoming these difficulties. This alternative fundamental solution is successfully applied towards solving the problem and is to be demonstrated as an efficient methodology. The final formulations are expressed explicitly and the dynamic effect of each wave is presented in a closed form. The results are valid for the infinitely many waves that are scattered from the crack tip and reflected by the free boundary. In some classes of dynamic problems, the ability to find a static field may hinge on waiting for the wave fronts to pass and the transient effect to die away. The characteristic time after which the transient effect can be neglected is also investigated in this study.

2 Required Fundamental Solutions

As usual in problems of the type considered here, superposition of solutions plays a significant role. The solutions to the problem considered in this study can be determined by superposition of the following problems. Problem A treats the dynamic concentrated force acting on a half-plane medium without a crack, which induces a traction on the planes that will eventually define the initial crack faces. In problem B, an infinite body containing a semi-infinite crack is considered in which the faces are subjected to tractions which are equal and opposite to those on the corresponding planes in problem A. Problem C considers a half-plane free surface subjected the incident waves which are generated by the crack in problem B. The reflected waves coming from the free boundary can be constructed by employing the method of images.

Problem B in the above-mentioned three fundamental problems is the only one which needs careful analysis. Reflected and diffracted waves are generated from physical considerations, thus eliminating the stress induced by incident waves on the traction-free boundaries of crack faces. For most of the dynamic problems, the incident waves can be represented in an exponential functional form in the Laplace transform domain of time. The reflected and diffracted waves generated by the crack can thus be constructed by the superposition method; that is, if the responses toward an applied exponentially distributed traction on the crack face in the Laplace transform domain can be obtained preliminarily. The superposition scheme proposed in this study, unlike usual superposition methods which are performed in the time domain, is performed in the Laplace transform domain.

This solution for an exponentially distributed loading applied to the crack faces in the Laplace transform domain will be referred to as the fundamental solution. The problem can be viewed as a half-plane problem with the material occupying the region $y \geq 0$, subject to the following boundary conditions:

$$\bar{\tau}_{yz}(x, 0, p) = e^{p\eta x} \quad -\infty < x < 0, \tag{1}$$

$$\bar{w}(x, 0, p) = 0 \quad 0 < x < \infty, \tag{2}$$

where p is the Laplace transform parameter and η is a constant. The overbar symbol is used for denoting the transform on time t. The governing equation can be represented by the two-dimensional wave equation

$$\frac{\partial^2 w}{\partial x^2} + \frac{\partial^2 w}{\partial y^2} = b^2 \frac{\partial^2 w}{\partial t^2}, \tag{3}$$

where b is the slowness of the transverse wave given by

$$b = 1/v = \sqrt{\rho/\mu},$$

in which $w(x, y, t)$ is the displacement normal to the xy-plane, v is the shear wave speed, and μ and ρ are the respective shear modulus and the mass density of the material. The nonvanishing shear stresses are

$$\tau_{yz} = \mu \frac{\partial w}{\partial y}, \quad \tau_{xz} = \mu \frac{\partial w}{\partial x}. \tag{4}$$

This problem can be solved by the application of integral transforms. Applying the one-sided Laplace transform over time, the two-sided Laplace transform over x under the restriction of $\mathrm{Re}(\eta) > \mathrm{Re}(\lambda)$, finally the Wiener-Hopf technique is implemented. The solutions of stresses and displacement for the boundary conditions (1) and (2) in the transform domain are

$$\bar{\tau}_{yz}(x, y, p) = \frac{1}{2\pi i} \int_{\Gamma_\lambda} \frac{(b+\lambda)^{1/2} e^{-p(\alpha y - \lambda x)}}{(b+\eta)^{1/2}(\eta - \lambda)} d\lambda, \tag{5}$$

$$\bar{\tau}_{xz}(x, y, p) = -\frac{1}{2\pi i} \int_{\Gamma_\lambda} \frac{\lambda e^{-p(\alpha y - \lambda x)}}{(b+\eta)^{1/2}(\eta - \lambda)(b-\lambda)^{1/2}} d\lambda, \tag{6}$$

$$\bar{w}(x, y, p) = -\frac{1}{2\pi i} \int_{\Gamma_\lambda} \frac{e^{-p(\alpha y - \lambda x)}}{\mu p (b+\eta)^{1/2}(\eta - \lambda)(b-\lambda)^{1/2}} d\lambda, \tag{7}$$

where

$$\alpha = (b^2 - \lambda^2)^{1/2}.$$

3 Transient Full-Field Analysis

The investigation of a subsurface crack subjected to dynamic loading is an important topic in material failure analysis. The problem considered here is an inclined semi-infinite crack located under the surface of a half-plane. Having two coordinate systems in the following analysis is convenient, since the surface of the half-plane is not parallel to the crack faces. The origins of the two coordinate systems $(\bar{x}, \bar{y})$ and (x, y) are both located at the crack tip as shown in Fig. 1. The planar crack lies in the plane $\bar{y} = 0$, $\bar{x} < 0$ and the inclined angle of the crack is ϕ. The coordinate transforms and stress relations between these two systems are

$$\bar{x} = x \cos\phi + y \sin\phi, \tag{8}$$

$$\bar{y} = -x \sin\phi + y \cos\phi, \tag{9}$$

$$\tau_{xz} = \tau_{\bar{x}\bar{z}} \cos\phi - \tau_{\bar{y}\bar{z}} \sin\phi, \tag{10}$$

$$\tau_{yz} = \tau_{\bar{x}\bar{z}} \sin\phi + \tau_{\bar{y}\bar{z}} \cos\phi. \tag{11}$$

This problem has a characteristic length. A direct attempt towards solving this problem by transform and Wiener-Hopf techniques is not applicable. The transient elastodynamic problem is solved by superposition of the fundamental solutions obtained in the previous section in the Laplace transform domain. The transient solutions are composed of an incident field, reflected field, and diffracted field, which are denoted by superscripts of i, r, and d, respectively. The incident wave is the response to loading applied to a semi-infinite unbounded medium. The reflected and diffracted waves are generated through application of an opposite traction at the crack surface thus eliminating the stress induced by incident wave.

Consider a half-plane body which is stress-free and at rest. At time $t = 0$, an anti-plane concentrated dynamic force is applied at the free surface of a half-plane at position (l, h). The time dependence of the loading is represented by the Heaviside step function $H(t)$. The incident fields in the Laplace transform domain can be obtained as follows:

$$\bar{w}^i(x, y, p) = \frac{1}{2\pi i}\int_{\Gamma_\lambda} \frac{1}{\mu p \alpha} e^{p[\alpha(y-h)+\lambda(x-l)]} d\lambda, \quad (12)$$

$$\bar{\tau}^i_{yz}(x, y, p) = \frac{1}{2\pi i}\int_{\Gamma_\lambda} e^{p[\alpha(y-h)+\lambda(x-l)]} d\lambda, \quad (13)$$

$$\bar{\tau}^i_{xz}(x, y, p) = \frac{1}{2\pi i}\int_{\Gamma_\lambda} \frac{\lambda}{\alpha} e^{p[\alpha(y-h)+\lambda(x-l)]} d\lambda. \quad (14)$$

The incident stress field $\bar{\tau}^i_{\bar{y}\bar{z}}(\bar{x}, 0, p)$ induced in the crack face at $\bar{y} = 0$ expressed in the $\bar{x} - \bar{y}$ coordinate system is

$$\bar{\tau}^i_{\bar{y}\bar{z}}(\bar{x}, 0, p) = \frac{1}{2\pi i}\int_{\Gamma_\lambda} e^{-p\alpha h_0 + p\lambda(\bar{x}-l_0)} d\lambda, \quad (15)$$

where

$$l_0 = l\cos\phi + h\sin\phi, \quad h_0 = -l\sin\phi + h\cos\phi.$$

The applied traction on the crack face, in order to eliminate the incident wave as indicated in (15) has the functional form $e^{p\lambda\bar{x}}$. Since the solutions of applying traction $e^{p\eta\bar{x}}$ on crack faces have been solved in Section 2, the reflected and diffracted fields generated from the inclined crack can be constructed by superimposing the incident wave traction that is equal and opposite to (15). When we combine Eqs. (5) and (15), the solution of reflected and diffracted waves for $\bar{\tau}_{\bar{y}\bar{z}}$ and $\bar{\tau}_{\bar{x}\bar{z}}$ in the Laplace transform domain can be expressed as follows:

$$\bar{\tau}^{d+r}_{\bar{y}\bar{z}}(\bar{x}, \bar{y}, p) = \frac{1}{4\pi^2}\int_{\Gamma_{\eta_1}}\int_{\Gamma_{\eta_2}} G(\eta_1, \eta_2) e^{-p(\alpha_1 h_0 + \eta_1 l_0)} \times e^{-p(\alpha_2\bar{y} - \eta_2\bar{x})} d\eta_2 d\eta_1, \quad (16)$$

$$\bar{\tau}^{d+r}_{\bar{x}\bar{z}}(\bar{x}, \bar{y}, p) = -\frac{1}{4\pi^2}\int_{\Gamma_{\eta_1}}\int_{\Gamma_{\eta_2}} \frac{\eta_2}{\alpha_2} G(\eta_1, \eta_2) e^{-p(\alpha_1 h_0 + \eta_1 l_0)} \times e^{-p(\alpha_2\bar{y} - \eta_2\bar{x})} d\eta_2 d\eta_1,$$

where

$$G(\eta_1, \eta_2) = \frac{(b+\eta_2)^{1/2}}{(b+\eta_1)^{1/2}(\eta_1 - \eta_2)},$$

$$\alpha_1 = (b^2 - \eta_1^2)^{1/2}, \quad \alpha_2 = (b^2 - \eta_2^2)^{1/2}.$$

The above solutions for stresses are expressed in the $\bar{x} - \bar{y}$ coordinate system. If the solutions are expressed in the $x - y$ coordinate system, then a small modification should be made to account the effect of coordinate transformation, and the result for $\bar{\tau}_{yz}$ is

$$\bar{\tau}^{d+r}_{yz}(x, y, p) = \frac{1}{4\pi}\int_{\Gamma_{\eta_1}}\int_{\Gamma_{\eta_2}} K_1(\eta_2) G(\eta_1, \eta_2) e^{-p(\alpha_1 h_0 + \eta_1 l_0)} \times e^{-p(\alpha_2\bar{y} - \eta_2\bar{x})} d\eta_2 d\eta_1,$$

where

$$K_1(\eta_2) = \cos\phi - \frac{\eta_2}{\alpha_2}\sin\phi.$$

Equation (16) constitutes a double inversion integral where the path Γ_{η_1} and Γ_{η_2} refer to Laplace inversion contours in the η_1-plane and the η_2-plane, respectively. The inverse transformation is carried out here through use of the Cagniard-de Hoop technique. Cagniard contours are introduced here in both η_1- and η_2-plane by setting

$$\alpha_1 h_0 + \eta_1 l_0 = t_1, \quad (17)$$

$$\alpha_2\bar{y} - \eta_2\bar{x} = t_2. \quad (18)$$

Equations (17) and (18) can be solved for η_1 and η_2 to yield

$$\eta_1^{\pm} = \frac{t_1\cos\Theta_0}{R_0} \pm i\frac{\sin\Theta_0}{R_0}(t_1^2 - b^2R_0^2)^{1/2}, \quad (19)$$

$$\eta_2^{\pm} = \frac{t_2\cos\psi}{d} \pm i\frac{\sin\psi}{d}(t_2^2 - b^2d^2)^{1/2}, \quad (20)$$

where (R_0, Θ_0) and (d, ψ) are the respective polar coordinates of the source point and field point, and

$$R_0 = (l_0^2 + h_0^2)^{1/2}, \quad \Theta_0 = \cos^{-1}(l_0/R_0),$$

$$d = (\bar{x}^2 + \bar{y}^2)^{1/2}, \quad \psi = \cos^{-1}(\bar{x}/d).$$

In the η_1-plane (or η_2-plane), (19) (or (20)) describes a hyperbola which is denoted as the Cagniard contour. The η_1- and η_2-integrations are then shifted onto Cagniard contours along which t_1 and t_2 are both real and positive. The two Cagniard contours must be superimposed in this technique for different locations of source and field points. Continuing from this, the reflected and diffracted waves can be automatically constructed. Because $G(\eta_1, \eta_2)$ possesses a pole at $\eta_1 = \eta_2$, the contribution of the pole has to be taken into account in the change of integral paths from η_1 to t_1 and η_2 to t_2. Recall from (16) that a pole term arises, representing the reflected waves. The contribution of this pole represents the reflected r wave generated from the crack surface. The reflected r waves can be concluded to pass the region for $\psi > \pi - \Theta_0$. By using the Cagniard-de Hoop method of Laplace inversion, reflected field in the time domain is obtained in a simple closed form

$$\tau^r_{yz}(x, y, t) = -\frac{t\sin\theta_1 H(t - br_1)}{\pi r_1(t^2 - b^2r_1^2)^{1/2}}, \quad (21)$$

where

$$r_1 = [(x-l_1)^2 + (y+h_1)^2]^{1/2}, \quad \theta_1 = \cos^{-1}\left(\frac{x-l_1}{r_1}\right),$$

$$l_1 = l\cos(2\phi) + h\sin(2\phi), \quad h_1 = l\sin(2\phi) - h\cos(2\phi).$$

The diffracted wave generated from the crack tip is considered next. Recalling that p is real and positive, the η_1- and η_2-integrations are shifted here onto Cagniard contours. The stress τ^d_{yz} induced by the diffracted wave from the crack tip is found to be

$$\tau^d_{yz}(x, y, t) = \frac{1}{2\pi^2}\int_{bR_0}^{t-bd} \mathrm{Re}\left[K_1(\eta_2^+)\left(G(\eta_1^+, \eta_2^+)\frac{\partial\eta_1^+}{\partial t_1}\frac{\partial\eta_2^+}{\partial t_2} - G(\eta_1^-, \eta_2^+)\frac{\partial\eta_1^-}{\partial t_1}\frac{\partial\eta_2^+}{\partial t_2}\right)\right] dt_1, \quad (22)$$

where

$$t_2 = t - t_1.$$

The incident shear wave (i wave) will generate a reflected wave (r wave) and a diffracted wave (d wave) from the subsurface crack. After some later time, these two waves are to reflect from the free half-surface which is to be indicated as the rr wave and dr wave. The solutions for rr and dr waves can be constructed by employing the method of images, which are easily obtained from the solutions of r and d waves, hence the results are omitted here. The reflected rr and dr waves will arrive at the crack tip at later time. The reflected waves (rrr and drr waves) and diffracted waves (rrd and drd waves) generated from the crack can be constructed following the previously indicated similar analysis.

The complete full-field solutions that account for the contributions of all the reflected and diffracted waves are finally

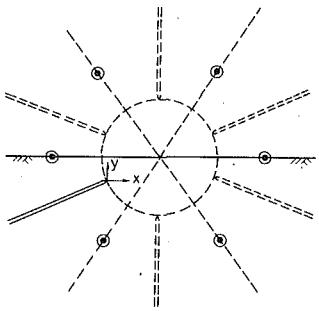

Fig. 2 Image method used to construct the transient full-field solutions

obtained explicitly. The image method shown in Fig. 2 is used for constructing the solution. The complete solutions for stresses and displacement can be simplified into a very compact form as follows:

$$\tau_{yz}=\sum_{i=0}^{s}\tau_{yz}^{i}+\sum_{k=0}^{n}\sum_{l=0}^{\infty}\sum_{j=0}^{m}\tau_{yz}^{j,k,l}, \tag{23a}$$

$$\tau_{xz}=\sum_{i=0}^{s}\tau_{xz}^{i}+\sum_{k=0}^{n}\sum_{l=0}^{\infty}\sum_{j=0}^{m}\tau_{xz}^{j,k,l}, \tag{23b}$$

$$w=\sum_{i=0}^{s}w^{i}+\sum_{k=0}^{n}\sum_{l=0}^{\infty}\sum_{j=0}^{m}w^{j,k,l}. \tag{23c}$$

The complete solutions consist of two terms as shown in (23). The first term with one summation is the contributions of incident wave and reflected waves which are only generated by reflected waves, i.e., $i = 0$ for incident wave, $i = 1$ for r wave, $i = 2$ for rr wave, $i = 3$ for rrr wave. The explicit forms are expressed as follows:

$$\tau_{yz}^{i}=(-1)^{i}\frac{t\sin\theta_i H(t-br_i)}{\pi r_i(t^2-b^2r_i^2)^{1/2}}, \tag{24a}$$

$$\tau_{xz}^{i}=-\frac{t\cos\theta_i H(t-br_i)}{\pi r_i(t^2-b^2r_i^2)^{1/2}}, \tag{24b}$$

$$w^{i}=\frac{1}{\pi\mu}\ln\left[\frac{t}{br_i}+\sqrt{\left(\frac{t}{br_i}\right)^2-1}\right]H(t-br_i), \tag{24c}$$

where

$$r_i=((x-l_i)^2+(y-h_i)^2)^{1/2},\quad \theta_i=\cos^{-1}\left(\frac{x-l_i}{r_i}\right),$$

$$l_0=l,\quad h_0=h,$$

$$l_1=l\cos(2\phi)+h\sin(2\phi),\quad h_1=l\sin(2\phi)-h\cos(2\phi),$$

$$l_i=l\cos((i+1)\phi)+h\sin((i+1)\phi)+\sum_{m=1}^{(i-1)/2}2h\sin(2m\phi),\quad i=3,5,7,\ldots$$

$$h_i=l\sin((i+1)\phi)-h\cos((i+1)\phi)-\sum_{m=1}^{(i-1)/2}2h\cos(2m\phi),\quad i=3,5,7,\ldots.$$

The second term in (23) with three summations comes from the contributions for diffracted waves and reflected waves which are generated by diffracted waves, i.e., $k = 0$, $l = 0$, $j = 0$ for d wave, $j = 1$ for dr wave, $j = 2$ for drr wave; $k = 0$, $l = 1$, $j = 0$ for drd wave, $j = 1$ for $drdr$ wave, $j = 2$ for $drdrr$ wave; $k = 0$, $l = 2$, $j = 0$ for $drdrd$ wave, $j = 1$ for $drdrdr$ wave; $k = 1$, $l = 0$, $j = 0$ for rrd wave, $j = 1$ for $rrdr$ wave; and $k = 1$, $l = 1$, $j = 0$ for $rrdrd$ wave, $j = 1$ for $rrdrdr$ wave. $k = 0$ can be seen here to consist of the diffracted d wave which is diffracted by the incident wave and the sequence of diffracted waves and reflected waves which are generated by the d wave. $k = 1$ consists of the diffracted rrd wave which is diffracted from the rr wave by the crack tip and the sequence of diffracted and reflected waves which are generated by the rrd wave. The index notation $j = 0$ will stand for the diffracted waves and $j \neq 0$ stands for the reflected waves. The results are expressed as follows:

$$\tau_{yz}^{j,k,l}=\frac{i^q}{2\pi^2(2\pi i)^l}\int_{bR_{0,2k}}^{a_1}\int_{2hb}^{a_2}\cdots\int_{2hb}^{a_{l+1}}\times FUN1_{j,k,l}\,dt_{k+l+1}dt_{k+l}\cdots dt_{k+1}, \tag{25a}$$

$$\tau_{xz}^{j,k,l}=\frac{-1}{2\pi^2(2\pi)^l}\int_{bR_{0,2k}}^{a_1}\int_{2hb}^{a_2}\cdots\int_{2hb}^{a_{l+1}}\times FUN2_{j,k,l}\,dt_{k+l+1}dt_{k+l}\cdots dt_{k+1}, \tag{25b}$$

$$w^{j,k,l}=\frac{-1}{2\pi^2(2\pi)^l\mu}\int_{bk}^{t}\int_{bR_{0,2k}}^{a_1'}\int_{2hb}^{a_2'}\cdots\int_{2hb}^{a_{l+1}'}\times FUN3_{j,k,l}\,dt_{k+l+1}dt_{k+l}\cdots dt_{k+1}, \tag{25c}$$

where

$$bk=b(R_{0,2k}+d_j+2lh),$$

$$a_1=t-bd_j-2lhb,\quad a_1'=\tau-bd_j-2lhb,$$

$$a_{v+1}=t-bd_j-t_1-t_2-\cdots-t_v-2(l-v)hb,\quad v=1,2,3,\ldots,l$$

$$a_{v+1}'=\tau-bd_j-t_1-t_2-\cdots-t_v-2(l-v)hb,\quad v=1,2,3,\ldots,l$$

$$FUN1_{j,k,l}=\mathrm{Op}\,(G(S_{2,k+1}^{\pm},\eta_{k+2}^{\pm})G(S_{2,k+2}^{\pm},\eta_{k+3}^{\pm})\cdots\times G(S_{2,k+2}^{\pm},\eta_{k+3}^{\pm})\cdots$$

$$\times\left(\pm\frac{\partial S_{2,k+1}^{\pm}}{\partial t_{k+1}}\right)\left(\pm\frac{\partial S_{2,k+2}^{\pm}}{\partial t_{k+2}}\right)\cdots\left(\pm\frac{\partial S_{2,k+l+1}^{\pm}}{\partial t_{k+l+1}}\right)\left(\frac{\partial S_{1,k+l+p+2}^{+}}{\partial t_{k+l+p+2}}\right)\Bigg),$$

$$l_i=l\cos(i\phi)+h\sin(i\phi)+\sum_{m=0}^{i/2-1}2h\sin(2m\phi),\quad i=2,4,6,\ldots$$

$$h_i=-l\sin(i\phi)+h\cos(i\phi)+\sum_{m=0}^{i/2-1}2h\cos(2m\phi),\quad i=2,4,6,\ldots$$

$$FUN2_{j,k,l}=\mathrm{Op}\left(\left(\frac{S_{1,l+k+p+2}^{+}}{(b^2-S_{1,l+k+p+2}^{+2})^{1/2}}\right)G(S_{2,k+1}^{\pm},\eta_{k+2}^{\pm})\times G(S_{2,k+2}^{\pm},\eta_{k+3}^{\pm})\cdots\times G(S_{2,k+l+1}^{\pm},\eta_{k+l+2}^{+})\left(\pm\frac{\partial S_{2,k+1}^{\pm}}{\partial t_{k+1}}\right)\right)$$

$$\times\left(\pm\frac{\partial S^{\pm}_{2,k+2}}{\partial t_{k+2}}\right).\ .\ .\ .\ .\left(\pm\frac{\partial S^{\pm}_{2,k+l+1}}{\partial t_{k+l+1}}\right)\left(\frac{\partial S^{+}_{1,k+l+p+2}}{\partial t_{k+l+p+2}}\right)\Bigg),$$

$$FUN3_{j,k,l}=\mathrm{Op}\left(\left(\frac{1}{(b^2-S^{+2}_{1,l+k+p+2})^{1/2}}\right)G(S^{\pm}_{2,k+1},\ \eta^{\pm}_{k+2})\right.$$

$$\times G(S^{\pm}_{2,k+2},\ \eta^{\pm}_{k+3}).\ .\ .\ .$$

$$\times G(S^{\pm}_{2,k+l+1},\ \eta^{+}_{k+l+2})\left(\pm\frac{\partial S^{\pm}_{2,k+1}}{\partial t_{k+1}}\right)\left(\pm\frac{\partial S^{\pm}_{2,k+2}}{\partial t_{k+2}}\right).\ .\ .\ .\ .$$

$$\left.\times\left(\pm\frac{\partial S^{\pm}_{2,k+l+1}}{\partial t_{k+l+1}}\right)\left(\frac{\partial \eta^{+}_{k+l+p+2}}{\partial t_{k+l+p+2}}\right)\right),$$

in which the operator "Op" is "Re" or "Im" depending on whether l is even or odd and

$$S^{+}_{1,k+l+p+2}=-\frac{t_{k+l+p+2}\cos\psi'_j}{s_j}+i\frac{\sin\psi'_j}{s_j}(t^2_{k+l+p+2}-b^2d^2_j)^{1/2},$$

$$S^{\pm}_{2,k+1}=\frac{t_{k+1}\cos\Theta_{0,2k}}{R_{0,2k}}\pm i\frac{\sin\Theta_{0,2k}}{R_{0,2k}}(t^2_{k+1}-b^2R^2_{0,2k})^{1/2},$$

$$S^{\pm}_{2,k+v+1}=\frac{t_{k+v+1}\sin\phi}{2h}\pm i\frac{\cos\phi}{2h}(t^2_{k+v+1}-4b^2h^2)^{1/2},$$

$$v=1,2,3,\ .\ .\ .\ ,l$$

$$\eta^{+}_{k+l+2}=-\frac{t_{k+l+2}\cos\psi_j}{d_j}+i\frac{\sin\psi_j}{d_j}(t^2_{k+l+2}-b^2d^2_j)^{1/2},$$

$$\eta^{\pm}_{k+v+1}=-\frac{t_{k+v+1}\sin\phi}{2h}\pm i\frac{\cos\phi}{2h}(t^2_{k+v+1}-4b^2h^2)^{1/2},$$

$$v=1,2,3,\ .\ .\ .\ ,$$

$S_{2,1}=\eta_1$, $t_{k+l+p+2}=t-t_{k+1}-t_{k+2}-.\ .\ .\ .\ .-t_{k+l+1}$,

$q=0$, when $l=0,2,4,6,\ .\ .\ .\ .\ .$; $q=1$,

when $l=1,3,5,7,\ .\ .\ .\ .\ .$

$p=j/2$, when $j=0,2,4,6,\ .\ .\ .\ .\ .$; $p=(j-1)/2$,

when $j=1,3,5,7,\ .\ .\ .\ .\ .$

$$R_{0,2k}=(l^2_{0,2k}+h^2_{0,2k})^{1/2};\ d_j=(x^2_j+y^2_j)^{1/2},$$

$$s_j=((x-l_j)^2+(y-h_j)^2)^{1/2};\ \cos\psi'_j=\frac{x-l_j}{s_j},$$

$$\cos\psi_j=\frac{x_j}{d_j};\ \cos\Theta_{0,2k}=\frac{l_{0,2k}}{R_{0,2k}},$$

$$l_{0,2k}=l\cos(2k+1)\phi+h\sin(2k+1)\phi+\sum_{m=0}^{k-1}2h\sin(2m+1)\phi,$$

$$h_{0,2k}=-l\sin(2k+1)\phi+h\cos(2k+1)\phi$$

$$+\sum_{m=0}^{k-1}2h\cos(2m+1)\phi,$$

$$x_j=(x-l_j)\cos(j+1)\phi+(y-h_j)\sin(j+1)\phi,$$

$$j=0,2,4,6,\ .\ .\ .\ .\ .$$

$$y_j=-(x-l_j)\sin(j+1)\phi+(y-h_j)\cos(j+1)\phi,$$

$$j=0,2,4,6,\ .\ .\ .\ .\ .$$

$$x_j=(x-l_j)\cos(j\phi)+(y-h_j)\sin(j\phi),\ j=1,3,5,7,\ .\ .\ .\ .\ .$$

$$y_j=-(x-l_j)\sin(j\phi)+(y-h_j)\cos(j\phi),$$

$$j=1,3,5,7,\ .\ .\ .\ .\ .$$

$l_0=0$; $h_0=0$,

$$l_j=\sum_{m=1}^{j/2}2h\sin(2m\phi),\ j=2,4,6,\ .\ .\ .\ .\ .$$

$$h_j=-\sum_{m=1}^{j/2}2h\cos(2m\phi),\ j=2,4,6,\ .\ .\ .\ .\ .$$

$$l_j=\sum_{m=0}^{(j-1)/2}2h\sin(2m\phi),\ j=1,3,5,7,\ .\ .\ .\ .\ .$$

$$h_j=\sum_{m=0}^{(j-1)/2}2h\cos(2m\phi),\ j=1,3,5,7,\ .\ .\ .\ .\ .$$

The number of reflected waves (i.e., n, s, and m) is dependent on the location and the inclined angle ϕ of the crack, and the position where the dynamic point loading is applied. The results are expressed as follows:

If $\phi_{2j+1}<\pi/2<\phi_{2j-1}$, then $n=j$.

If $(2v-1)\phi<\phi_{2n+1}<2v\phi$, then $s=2(n+v)+1$.

If $2v\phi<\phi_{2n+1}<(2v+1)\phi$, then $s=2(n+v)+2$.

If $(2v-1)\phi<\pi/2<2v\phi$, then $m=2v$.

If $2v\phi<\pi/2<(2v+1)\phi$, then $m=2v+1$

where

$$\phi_{2j+1}=\cos^{-1}\left(\frac{l_{2j+1}}{R_{2j+1}}\right),$$

$$R_{2j+1}=(l^2_{2j+1}+h^2_{2j+1})^{1/2},$$

$$l_{2j+1}=l\cos2(j+1)\phi+h\sin2(j+1)\phi+\sum_{p=1}^{j}2h\sin(2p\phi),$$

$$h_{2j+1}=l\sin2(j+1)\phi-h\cos2(j+1)\phi-\sum_{p=1}^{j}2h\cos(2p\phi).$$

4 Numerical Results of Transient Solutions

The geometric configuration considered in this study is an inclined semi-infinite crack located under the surface of a half-plane. The incident wave generated by the dynamic antiplane loading will be diffracted from the crack tip and reflected from the crack surface as d and r waves, which will be reflected from the half-plane and interact with the inclined crack again at later time. The complete structure of the wave fronts for the incident, reflected, and diffracted waves over a short time period are expressed in Fig. 3.

The exact full-field solutions have been determined in the previous section. The transient response for a point dynamic

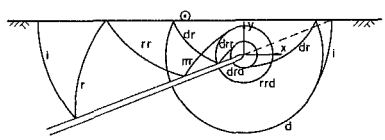

Fig. 3 Wave fronts of the incident, reflected, and diffracted waves for a short time period after the impact loading is applied on the half-space

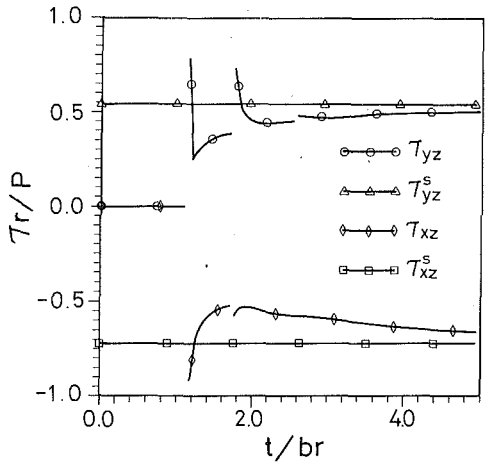

Fig. 4 Transient shear stresses for the field point located at $r = 5$, $\theta = 30$ deg due to impact loading applied at $(-25, 10)$

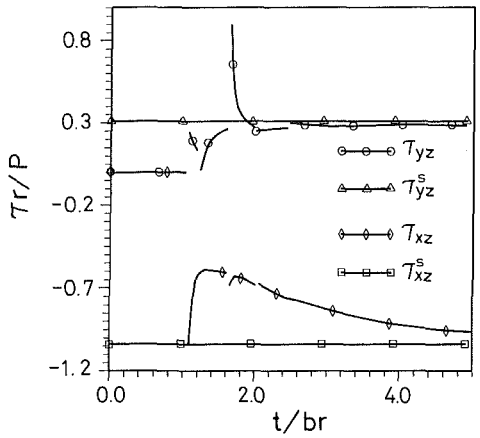

Fig. 5 Transient shear stresses for the field point located at $r = 5$, $\theta = 60$ deg due to impact loading applied at $(-25, 10)$

loading is next investigated here with a Heaviside function $H(t)$ time dependence and with a magnitude P applied at $(-25, 10)$ which is at the left-hand side of the crack tip. The inclined angle ϕ of the crack is chosen to be 30 deg and the shear wave speed is assumed to be 3200 m/sec. It is worthy to note that only the incident wave and the second reflected *rr* wave will pass through the crack tip and generate a sequence of diffracted waves; the other pure reflected waves (i.e., *rrr*, *rrrr*, etc.) will only reflect back and forth between the crack face and the half-plane surface. Hence, in this particular case, k is equal to 0 and 1 and the associated wave fronts are shown in Fig. 3. The field points located at $r = 5$, $\theta = 30$ deg, 60 deg, and 120 deg are selected for analyzing the transient response. The transient shear stresses of these points are expressed in Figs. 4–6. The time has been normalized by dividing *br*. The corresponding static solutions are also indicated in these figures. The incident and purely reflected waves are singular at their wave fronts while the diffracted waves have finite jumps at their wave fronts. In these figures the transient stresses tend toward the corresponding static value after the third diffracted wave has passed the field points. Next, we consider the point loading being applied directly above the crack tip, so that $l = 0$ and $h = 10$. The field points to be investigated are at $r = 5$, $\theta = 0$ deg and 120 deg. In this case, only the incident wave will generate a sequence of diffracted waves, hence $k = 0$. The transient shear stresses are plotted in Figs. 7–8. It is indicated in these figures that after the second diffracted wave has passed, the transient stresses will approach the static value.

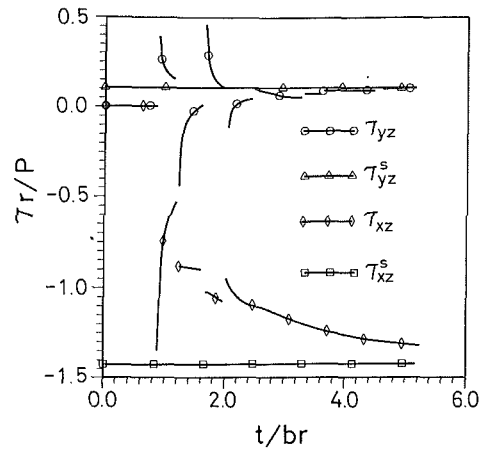

Fig. 6 Transient shear stresses for the field point located at $r = 5$, $\theta = 120$ deg due to impact loading applied at $(-25, 10)$

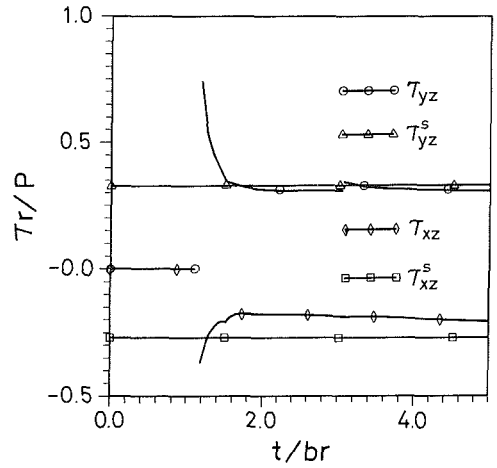

Fig. 7 Transient shear stresses for the field point located at $r = 5$, $\theta = 0$ deg due to impact loading applied at (0, 10)

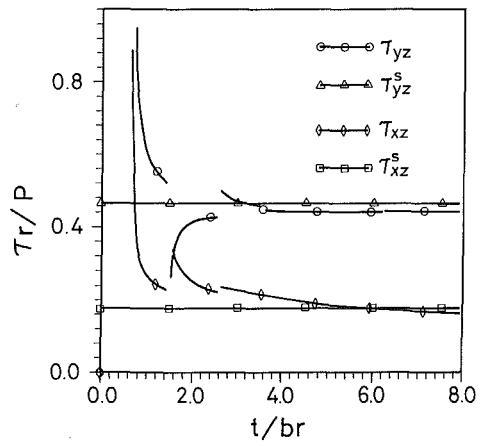

Fig. 8 Transient shear stresses for the field point located at $r = 5$, $\theta = 120$ deg due to impact loading applied at (0, 10)

5 Conclusions

Most of the problems which have been studied in the development of fracture mechanics are quasi-static. Because of

loading conditions and material properties, numerous problems have existed for which the assumption of quasi-static deformation is invalid, and the inertia of the material must be taken into account. It would be difficult to state precise conditions under which inertia effects might be neglected. The propagation of stress waves through an unbounded medium has not been a difficult subject. However, if boundaries are introduced, reflected and diffracted waves will be generated from boundaries, making the problem much more complicated.

The transient response of a half-space containing a subsurface inclined crack has been considered here to gain understanding of the interaction of stress waves with material defects. This problem contains a characteristic length and is solved by superposition of the fundamental solutions in the Laplace transform domain. The exact transient full-field solutions for stresses and displacement over a long period of time are obtained in this study. The complicated close-form transient solutions are expressed in a very simple formulation which account for all contributions coming from incident, reflected, and diffracted waves. The transient stresses near the crack tip can be used for analyzing the condition for unstable crack propagation. The transient displacement responses at the half-plane surface could possibly be used to detect the location of the subsurface crack and its orientation.

One of the main objectives in this study is to investigate the characteristic time in which the transient solution would approach the correspondent static value in dynamic fracture problems. With the exact analytic solutions at hand, numerical calculations for the transient stresses have been presented and compared to corresponding static values. It is found in this study that the transient effect in this problem can be neglected after the first few diffracted waves being generated from the crack tip have passed the field points.

Acknowledgments

The research support of the National Science Council, Republic of China, through Grant NSC 81-0401-E002-18 at National Taiwan University is gratefully acknowledged.

References

Brock, L. M., 1982, "Shear and Normal Impact Loadings on One Face of a Narrow Slit," *International Journal of Solids and Structures*, Vol. 18, pp. 467–477.

Brock, L. M., 1984, "Stresses in a Surface Obstacle Undercut Due to Rapid Indentation," *Journal of Elasticity*, Vol. 14, pp. 415–424.

Brock, L. M., Jolles, M., and Schroedl, M., 1985, "Dynamic Impact Over a Subsurface Crack: Applications to the Dynamic Tear Test," ASME JOURNAL OF APPLIED MECHANICS, Vol. 52, pp. 287–290.

Brock, L. M., 1986, "Transient Dynamic Green's Functions for a Cracked Plane," *Quarterly of Applied Mathematics*, Vol. 44, pp. 265–275.

de Hoop, A. T., 1958, "Representation Theorems for the Displacement in an Elastic Solid and Their Application to Elastodynamic Diffraction Theory," Doctoral Dissertation, Technische Hoegschool, Delft, The Netherlands.

Freund, L. B., 1974, "The Stress Intensity Factor Due to Normal Impact Loading of the Faces of a Crack," *International Journal of Engineering Science*, Vol. 12, pp. 179–189.

Lee, Y. J., and Freund, L.B., 1990, "Fracture Initiation Due to Asymmetric Impact Loading of an Edge Cracked Plate," ASME JOURNAL OF APPLIED MECHANICS, Vol. 57, pp. 104–111.

Ma, C. C., and Chen, S. K., 1993, "Exact Transient Analysis of an Antiplane Semiinfinite Crack Subjected to Dynamic Body Forces," *Wave Motion*, Vol. 17, pp. 161–171.

Ma, C. C., and Hou, Y. C., 1990, "Theoretical Analysis of the Transient Response for a Stationary Inplane Crack Subjected to Dynamic Impact Loading," *International Journal of Engineering Science*, Vol. 28, pp. 1321–1329.

Ma, C. C., and Hou, Y. C., 1991, "Transient Analysis for Antiplane Crack Subjected to Dynamic Loadings," ASME JOURNAL OF APPLIED MECHANICS, Vol. 58, pp. 703–709.

Noble, B., 1958, *The Wiener-Hopf Technique*, Pergamon Press, New York.

Tsai, C. H., and Ma, C. C., 1992, "Transient Analysis of a Semi-infinite Crack Subjected to Dynamic Concentrated Forces," ASME JOURNAL OF APPLIED MECHANICS, Vol. 59, pp. 804–811.